SIMULATION STUDY ON SOYBEAN WINNOWING BASED ON CFD-DEM COUPLING

, CFD-DEM 耦合的大豆风选仿真研究

Guangwei CHEN 1), Fuxing LI1), FaYi QU*2), ChongJian ZHANG1)

¹⁾Northeast Forestry University, College of Mechanical and Electrical Engineering, Harbin / China; ²⁾Northeast Forestry University, Graduate School, Harbin / China. *Tel:* +86 15663693373; *E-mail: fuxingli07@gmail.com DOI: https://doi.org/10.35633/inmateh-77-29*

Keywords: Soya cleaning, CFD-DEM coupling, simulation analysis, air winnowing

ABSTRACT

To address the issues of high impurity content and seed loss in soybean cleaning, this study employs a CFD–DEM coupled simulation using SN52 soybeans and a single-factor experimental design to analyze the air winnowing process under different inclination angles, inlet air velocities, and inlet opening sizes. The results indicate that, at an inlet air velocity of 17 m/s and an inlet opening size of 220 mm, the impurity rate decreases with increasing inclination angle, while the loss rate first decreases and then increases. When the inclination angle is 21° and the inlet opening size is 220 mm, the impurity rate decreases with increasing inlet air velocity, with the loss rate again showing an initial decrease followed by an increase. Similarly, at a 21° inclination angle and an inlet air velocity of 17 m/s, the impurity rate decreases as the inlet opening size increases, while the loss rate exhibited the same initial decrease and subsequent increase. The optimal parameter combination is determined to be 17 m/s inlet air velocity, 21° inclination angle, and 220 mm inlet opening size, achieving an impurity rate of 1.59%, a loss rate of 0.26%, and a cleaning efficiency of 98.15%. These findings provide a theoretical basis for the optimized design of airflow-based soybean cleaning equipment.

摘要

针对大豆清洗过程中含杂率高与损失率大的问题,本研究以 SN52 大豆为研究对象,采用 CFD-DEM 耦合模拟与单因素控制变量法,模拟了不同倾角、风速及进风口尺寸下的风选过程。结果表明:在风速 17 m/s、进风口尺寸 220 mm 时,含杂率随倾角增大而降低,损失率则呈现先下降后上升的趋势;在倾角 21°、进风口尺寸 220 mm 时,含杂率随风速增大而降低,损失率同样呈现先降后升的趋势;在倾角 21°、风速 17 m/s 时,含杂率随进风口尺寸增大而降低,损失率亦呈现先下降后上升的规律。综合数据表明,最优参数组合为风速 17 m/s、倾角 21°、进风口尺寸 220 mm,此时含杂率为 1.59%,损失率为 0.26,清洗效率达 98.15%。研究结果可为气流式大豆风选设备的优化设计提供理论依据。

INTRODUCTION

As an essential source of protein, edible oil, and livestock feed, soybean is widely cultivated worldwide and represents an indispensable crop in agricultural production (*Toomer et al.*, 2023). Field observations during cultivation and harvest reveal that multi-variety planting and natural variations in soybean seed dimensions result in complex mixtures containing beans of varying quality alongside impurities such as stones and straw fragments (*Chen et al.*, 2019). Since all components except stones retain value for utilization, cleaning is essential to enable targeted applications. Current crop cleaning equipment mainly employs two approaches: systems integrating vibrating screens with air blowers, and those utilizing pneumatic separation based on differences in density or suspension velocity between grains and impurities (*Krzysiak et al.*, 2020). The latter's screenless design avoids material damage while offering benefits in structural simplicity, reduced failure rates, and easier maintenance. Although pneumatic cleaning has matured in walnut processing, waste sorting, and tea production, systematic research on airflow-based systems specifically adapted to soybean materials remains limited (*Nahal et al.*, 2013; *Zhao et al.*, 2021; *Xie et al.*, 2022). With progress in cleaning technology and rapid advances in computer science, researchers have introduced CFD-DEM coupled simulation to analyze particle movement and behavior in airflow fields.

Guang Wei CHEN Assoc. Prof.; Fuxing LI, Postgraduates.; FaYi QU, Assistant Research Fellow; Chong Jian ZHANG, Postgraduates.

This method not only enables visual observation of inter-particle interactions but also lowers trial-anderror costs and overcomes spatiotemporal constraints, leading to its broad adoption in pneumatic separation applications.

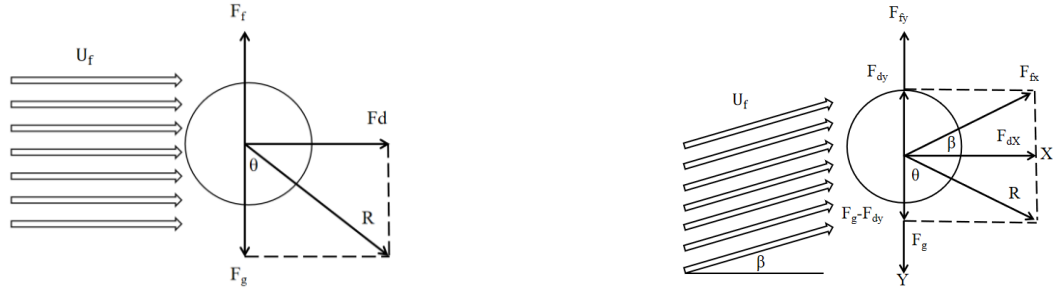
Earlier researchers pioneered the application of gas-solid coupled simulation in the analysis of particle motion within pipelines, revealing wave-like diffusion patterns along the flow boundaries and establishing collision dynamics equations, thereby providing a foundation for studying the behavior of irregular particles in airflow systems using gas-solid coupling (Tsuji et al., 1993). In subsequent work, differences in energy consumption and airflow requirements for achieving the same separation effect between rapeseed and lightweight impurities under horizontal and vertical airflow configurations were examined. The results showed that horizontal airflow required lower energy input and reduced airflow volume compared to vertical airflow (Moses et al., 2014). To address uneven flow velocity and spatial limitations in rice air separation devices, Du et al. (2014) employed CFD-DEM coupled simulation to analyze collision behavior and motion trajectories of grain mixture particles, thereby guiding the structural optimization of the air separation chamber. Subsequently, Zhao et al. (2020) investigated the problem of inefficient primary separation of husk and brown rice by examining particle-airflow interactions within the flow field, revealing how brown rice loss and husk residue varied with different airflow distributions. In addition, Hu et al. (2020) analyzed the motion characteristics of material and impurity particles during saffron cleaning using CFD-DEM simulation, identifying airflow velocity, inclination angle, and dust removal port angle as key operational and structural parameters influencing the separation efficiency of the airflow cleaning device.

In this study, an airflow-based soybean cleaning device is designed based on the principles of air winnowing and aerodynamics, and a CFD–DEM coupled simulation is employed to analyze the movement behavior of seeds and impurities during the separation process. The effects of inlet air velocity, inclination angle, and inlet opening size on separation efficiency are evaluated, and the corresponding impacts on impurity rate and seed loss rate are clarified. Based on these results, an optimization scheme for the air separation chamber structure and operating parameters under single-factor conditions is proposed, providing a basis for further research and performance improvement.

MATERIALS AND METHODS

Selection of airflow cleaning method and modelling of soybean winnowing chamber

The force analysis of the inclined and horizontal airflow is shown in e.g. 1. In both airflow modes of action, the particulate material is subject to the combined action of gravity F_g , buoyancy F_f and airflow trailing force F_d . Among them, the combined force R of F_d and F_f forms an angle θ in the direction of particle movement with gravity F_g . Under the condition of horizontal airflow, the distance of particle movement is prolonged with the increase of θ angle; while in the inclined airflow, in addition to the role of θ angle, the direction of the airflow and the horizontal plane forms β angle, which not only makes the material generate the force in the direction of the y-axis, but also prolongs the retention time of the material in the sorting area, which improves the accuracy and efficiency of the sorting ($Zhang\ et\ al.,\ 2020$). Based on this, this paper intends to construct an air separation chamber model for the tilted airflow sorting mechanism and study its sorting performance.



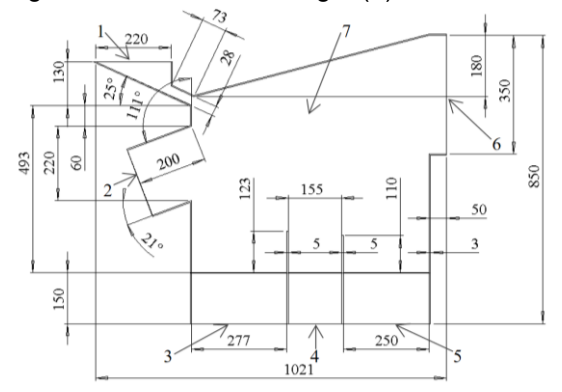
a- Horizontal airflow pattern force analysis diagram

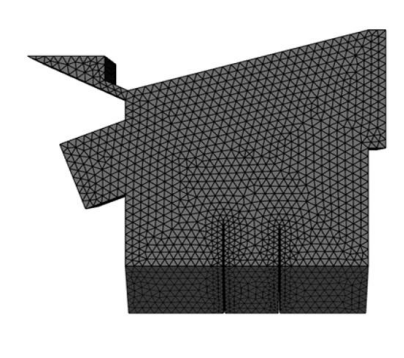
b- Inclined airflow pattern force analysis diagram

Fig. 1 - Force analysis diagrams for horizontal and inclined airflow patterns

Considering the characteristics of the inclined airflow and the separation requirements of the soybean mixture, the soybean air winnowing device designed in this study consists of seven main components: a material inlet, an air inlet, four material outlets (I–IV), and the winnowing chamber. Outlet IV also serves as an auxiliary air inlet. To improve CFD–DEM coupling efficiency and avoid numerical dispersion, the structure of the device was geometrically simplified. The simplified geometry and corresponding dimensional parameters are shown in Fig. 2(a).

A simplified three-dimensional model of the air separation chamber was constructed in SolidWorks and exported in .x-t format for import into the meshing module of Fluent. Boundary conditions were then defined as follows: material inlet 1, primary air inlet 2, outlet for heavy impurities 3, outlet for large soybeans 4, outlet for small soybeans 5, and outlet for light impurities 6, which also functions as the exhaust air outlet. The mesh was generated with a minimum element size of 15 mm and a maximum element size of 25 mm, and the average mesh quality exceeded 0.85, meeting the accuracy requirements of subsequent simulations. The meshing results are shown in Fig. 2(b).





a- Models and main dimensions of winnowing device

b- Grid of air winnowing device

1. Material inlet; 2. Air inlet; 3. Material outlet I; 4. Material outlet II; 5. Material outlet III; 6. Material outlet IV 7. Winnowing chamber

Fig. 2 - Soybean air winnowing device main dimensions and computational grid

Establishment of the simulation model and force analysis

The experimental materials were sourced from the second accumulated temperature zone of Heilongjiang Province, China. The SN52 soybean mixture, which has a large regional planting area, was selected for the study. The mixture was classified into four categories: heavy impurities, plump large soybeans, small (underdeveloped) soybeans, and light impurities. Representative samples of each category are shown in Fig. 3.



a- Heavy impurities



b- Plump large soybeans



c- Underdeveloped small soybeans



d- Light impurities

Fig. 3 - Physical characteristics of the soybean mixture

In this study, the simulated particle models were constructed based on the measured physical characteristics of the collected materials, as shown in Fig. 4. Heavy impurities were represented using EDEM's built-in tetrahedral particle shape with a radius of 3.6 mm for default filling. Plump large soybeans and underdeveloped small soybeans were modeled using single-sphere particles with radii of 3.745 mm and 2.67 mm, respectively. Light impurities were represented using EDEM's straight tetrahedral particle shape, with a length of 5 mm and a radius of 1 mm for default filling.



a- Heavy impurities



b- Plump large soybeans



c- Underdeveloped small soybeans



d- Light impurities

Fig. 4 - Simulated particle models of the soybean mixture

Because the density, mass, and aerodynamic surface area of heavy impurities, plump large soybeans, underdeveloped small soybeans, and light impurities are different, the particles follow different motion trajectories when subjected to the inclined airflow. As shown in Fig. 5, when the airflow inclination angle $\theta = (0, \pi/2)$, the landing position of the particles is inversely related to their mass. Heavy impurities and plump large soybeans settle into Outlet I and Outlet II, respectively; light impurities are carried out of the chamber along the airflow direction; and underdeveloped small soybeans fall into Outlet III.

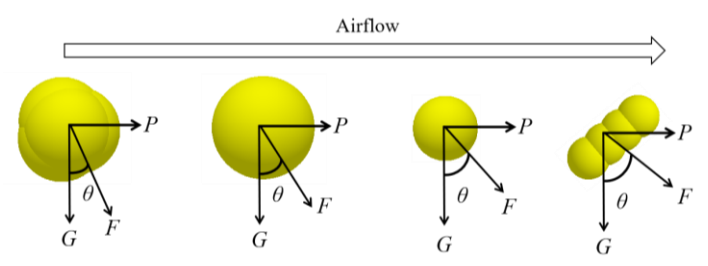


Fig. 5 - Simulation model force analysis

CFD-DEM simulation for evaluation of air separation performance and parameter settings

The main performance indicators of the soybean air winnowing device are the impurity rate (Y_1) and the loss rate (Y_2) of the soybeans after separation. Therefore, the impurity rate Y_1 and the loss rate Y_2 are selected as the performance evaluation indices of the device.

Outlet II is designated as the discharge port for plump large soybeans. The impurity rate of the material collected at Outlet II is calculated using Eq. (1).

$$Y_{1} = \frac{N_{s} + N_{X} + N_{q}}{N} \times 100\% \tag{1}$$

where: N_s - number of heavy impurities at Outlet II, [pcs]; N_x - number of underdeveloped small soybeans at Outlet II, [pcs]; N_q -- number of light impurities at Outlet II, [pcs]; N_q - total number of particles collected at Outlet II, [pcs].

The loss rate of plump large soybeans is determined by calculating the mass of intact soybeans discharged into Outlets I and III. The loss rate is calculated using Eq. (2).

$$Y_2 = \frac{M_1 + M_3}{M_1 + M_2 + M_3} \times 100\% \tag{2}$$

where: M_I - mass of plump large soybeans discharged to Outlet I, [kg]; M_2 - mass of plump large soybeans collected at Outlet II, [kg]; M_3 - mass of plump large soybeans discharged to Outlet III, [kg].

Compression and tensile tests were conducted on the four groups of soybean materials using a CTM2500 universal testing machine to determine their Poisson's ratios and shear moduli. Density was measured using an electronic balance combined with the cylinder water displacement method. The frictional contact parameters between each material group and acrylic were obtained through inclined plate tests, using sliding and rolling measurement methods, respectively. The mechanical property parameters and the contact coefficients used in the EDEM simulation are listed in Tables 1 and 2. The soybean air-winnowing and separation device is made of acrylic (*Zhu et al., 2024; Thiet et al., 2020; Chen et al., 2024*).

Physical parameters of soybean mixture materials and acrylic

Table 1

Material	Heavy impurities	Plump large soybean	Underdeveloped small soybean	Light impurities	Acrylic
Poisson ratio	0.18	0.25	0.21	0.32	0.3
Modulus of shear/Pa	1e+08	6.425e+07	5.627e+07	1.1e+9	1e+07
Density / (kg/m³)	2700	1285	1168	520	1200

Contact coefficients of material particles and acrylic

Table 2

Material	Restitution coefficient	Static friction coefficient	Sliding friction coefficient
Heavy impurities - heavy impurities	0.4	0.36	0.01
Heavy impurities - acrylic	0.3	0.4	0.01
Plump large soybeans - plump large soybeans	0.25	0.26	0.02
Plump large soybeans - acrylic	0.483	0.384	0.0275
Underdeveloped small soybeans - underdeveloped small soybeans	0.25	0.248	0.05
Underdeveloped small soybeans - acrylic	0.563	0.451	0.038
Light impurities - light impurities	0.35	0.40	0.042
Light impurities - acrylic	0.45	0.32	0.1

The quantity ratio of plump large soybeans, heavy impurities, underdeveloped small soybeans, and light impurities was set to 7.5:0.5:1:1, and a total of 2,000 particles were generated per second according to this proportion. The time step in EDEM was set to 4e-07, and the calculation in FLUENT was performed using a transient solver with a time step of 1×10⁻⁴ s, resulting in a 250:1 time-step coupling ratio between FLUENT and EDEM. Maintaining an integer multiple ratio between the two time steps is essential to ensure the stability and accuracy of the CFD-DEM coupling. The DDPM coupling interface was used to achieve two-way interaction between the airflow field and the particle phase. After completing the above parameter settings, the CFD-DEM coupled simulation was executed.

RESULTS

Analysis of evaluation indexes of soybean air separation effect in EDEM simulation

In the EDEM simulation, Outlet I and Outlet III were defined as the statistical regions for calculating the soybean loss rate, and the number of particles passing through these outlets during the simulation period (0–3 s) was recorded. Outlet II was defined as the statistical region for calculating the soybean impurity rate, and the mass of different particle types passing through Outlet II within 0–3 s was collected. The statistical regions used for performance evaluation are shown in Fig. 6.

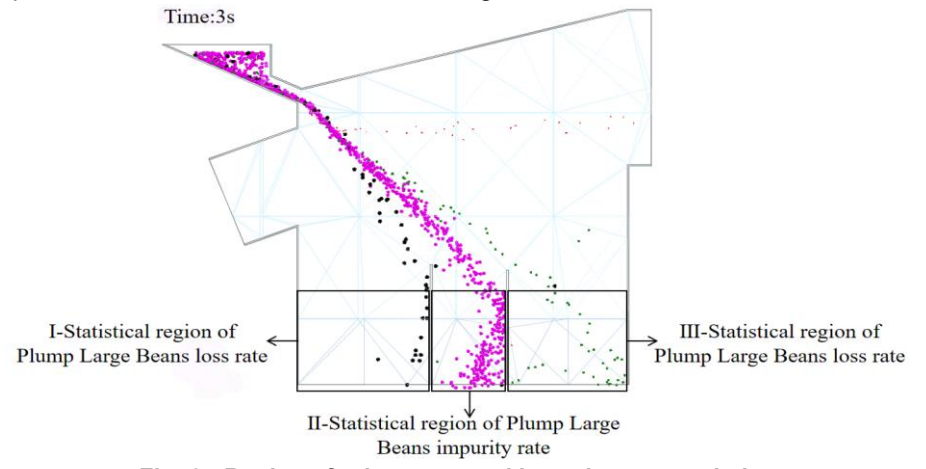


Fig. 6 - Regions for loss rate and impurity rate statistics

Influence of airflow inclination on soybean air winnowing performance

As shown in Fig. 7, transient particle motion snapshots were obtained at an inlet air velocity of 17 m/s and an inlet opening size of 220 mm under airflow inclination angles of 15°, 18°, 21°, and 24°. When the inclination angle was 15°, some underdeveloped small soybeans collided with the baffles and mixed with the plump large soybeans, causing both to fall into the same outlet. In addition, the light impurities did not obtain sufficient lift height and were only partially discharged from the chamber. As the inclination angle increased, the flight height and horizontal displacement of the particles increased, and collisions between particles and the baffle were reduced. Consequently, light impurities were more effectively drawn toward the exhaust outlet, and the separation accuracy of each particle group improved. However, when the inclination angle reached 24°, the forward motion of plump large soybeans and heavy impurities became excessive, causing some particles to enter incorrect outlets. Overall, the airflow inclination angle is positively correlated with particle flight height and travel distance. Therefore, selecting an appropriate inclination angle is essential to ensure accurate material separation and minimize both impurity rate and loss rate during soybean air winnowing.

Fig. 8 shows the particle force distribution and velocity field contours under airflow inclination angles of 15°, 18°, 21°, and 24°, with the inlet air velocity set to 17 m/s and the inlet opening size set to 220 mm. As shown in the figure, the maximum airflow velocity near the air inlet corner increases slightly with increasing inclination angle; however, this change does not substantially affect the overall airflow rate or the internal flow field structure of the air separation chamber. As the inclination angle increases, the airflow direction within the chamber shifts upward, resulting in an upward displacement of the particle force region. This change corresponds to the increased particle travel distance and flight height observed in the EDEM particle motion simulations.

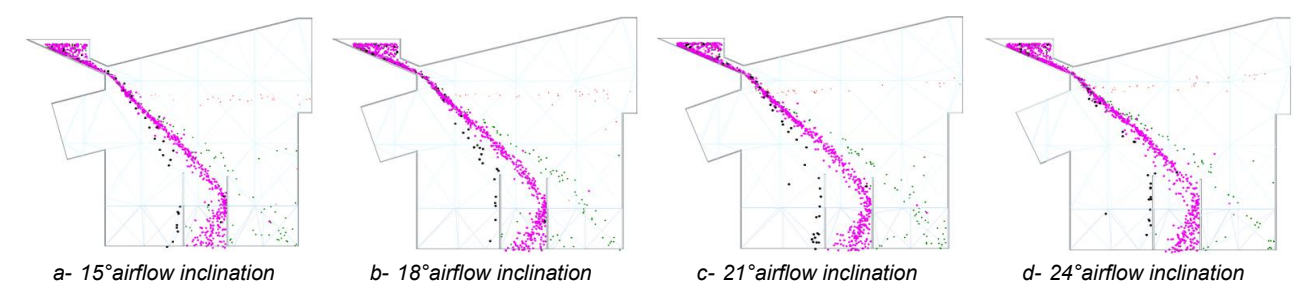


Fig. 7 - Particle motion snapshots under different airflow inclination angles

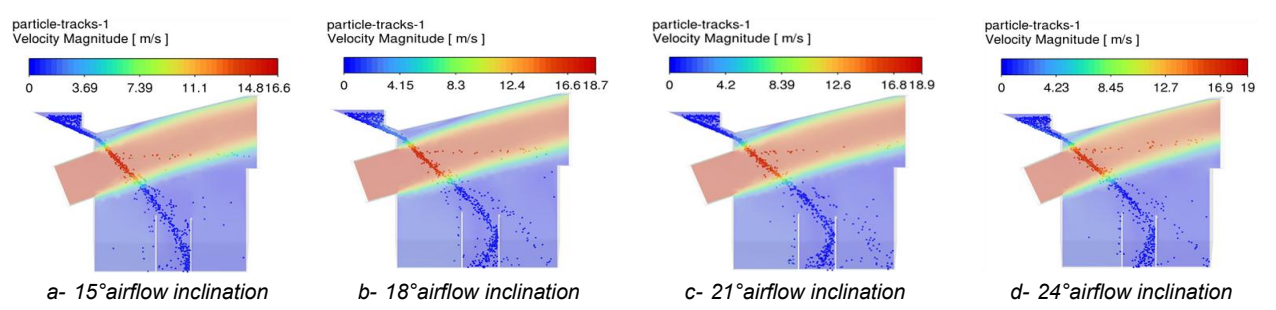


Fig. 8 - Particle force distribution and velocity field contours under different airflow inclination angles

At an inlet air velocity of 17 m/s, an inlet opening size of 220 mm, and an airflow inclination angle of 15°, the soybean air separation device achieved a loss rate of 0.29%, an impurity rate of 2.35%, and a cleaning efficiency of 97.36%. As the inclination angle increased, the impurity rate decreased continuously, while the loss rate first decreased and then increased. The overall fluctuation in cleaning efficiency remained within approximately 0.5%. The simulation results for loss rate, impurity rate, and cleaning efficiency under different inclination angles are summarized in Table 4. To more clearly illustrate the variation trends, the data are plotted in Fig. 9.

In summary, changes in airflow inclination do not markedly alter the overall structure of the internal flow field, but they do influence the airflow direction, which in turn has a significant effect on particle motion and separation performance. Considering the impurity rate, loss rate, and overall cleaning efficiency under the four inclination conditions, it can be concluded that, at an inlet air velocity of 17 m/s and a feeding rate of 2000 particles/s, airflow inclination angles between 18° and 24° yield satisfactory separation results. Among them, an inclination angle of 21° provides the best cleaning performance under the current parameter settings.

Table 3
Numerical simulation results with different airflow inclinations

Airflow inclination (°)	Impurity rate (%)	Loss rate (%)
15	2.35	0.29
18	2.27	0.23
21	1.59	0.26
24	1 44	0.69

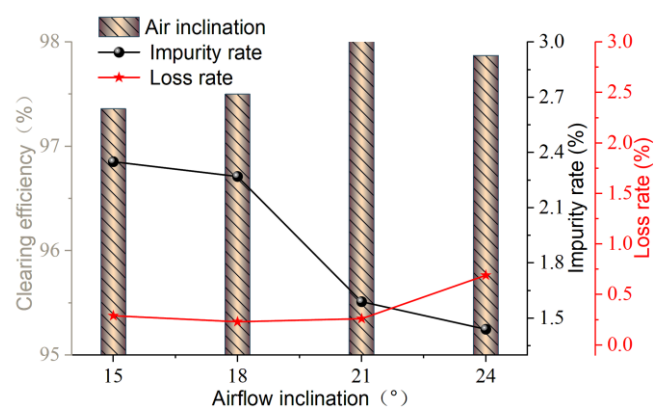


Fig. 9 - Trends of impurity rate and loss rate under different airflow inclination angles

Influence of airflow velocity on the effectiveness of soybean air winnowing

As shown in Fig. 10, particle motion snapshots were obtained at an airflow inclination angle of 21° and an inlet opening size of 220 mm, under inlet air velocities of 15, 16, 17, and 18 m/s. When the inlet air velocity was 15 m/s, frequent collisions occurred between plump large soybeans and the baffle between Outlets I and II, resulting in the misclassification of some underdeveloped small soybeans together with the plump large soybeans. In addition, the flight height of the light impurities was insufficient, causing part of the light impurities to remain in the chamber rather than being discharged through the exhaust outlet.

As the inlet air velocity increased from 15 m/s to 17 m/s, collisions between the particles and the baffle were gradually reduced, and the flight height of the light impurities increased, allowing the materials to fall more accurately into their corresponding outlets. However, when the inlet air velocity reached 18 m/s, the horizontal movement distance of the plump large soybeans and heavy impurities became excessive, causing renewed collisions with the baffle. As a result, some plump large soybeans and heavy impurities were misdirected away from their designated outlets, while the light impurities tended to converge toward the central outlet region. Therefore, to minimize particle-baffle collisions and ensure accurate separation, the inlet air velocity should not be too high or too low. An appropriate inlet air velocity is essential to achieve stable and effective air winnowing performance.

Fig. 11 shows the particle force distribution and airflow velocity contours at an airflow inclination angle of 21°, an inlet opening size of 220 mm, and a particle feeding rate of 2000 particles/s, under inlet air velocities of 15, 16, 17, and 18 m/s. As shown in the figure, as the inlet air velocity increases, the maximum airflow velocity near the inlet corner increases slightly and the overall airflow intensity in the chamber increases accordingly. However, the general structure of the airflow field does not change significantly, and the location of the dominant particle force region within the flow field remains essentially unchanged.

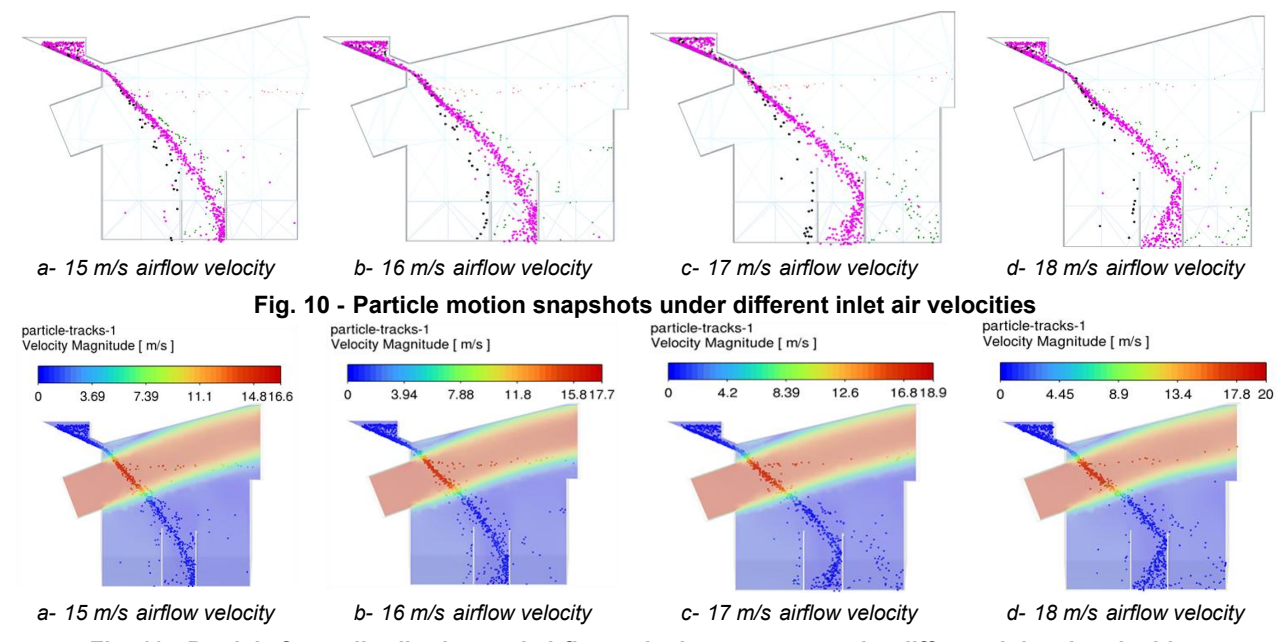


Fig. 11 - Particle force distribution and airflow velocity contours under different inlet air velocities

At an airflow inclination angle of 21° and a feeding rate of 2000 particles/s, the separation performance varied with inlet air velocity. When the inlet air velocity was 15 m/s, the loss rate, impurity rate, and cleaning efficiency were 2.46%, 11.65%, and 85.89%, respectively. Increasing the velocity to 16 m/s reduced the loss rate to 0.55% and the impurity rate to 6.75%, resulting in a cleaning efficiency of 92.70%. When the inlet air velocity reached 17 m/s, optimal separation performance was obtained, with a loss rate of 0.26%, an impurity rate of 1.59%, and a cleaning efficiency of 98.15%. However, further increasing the velocity to 18 m/s caused the loss rate to rise to 1.55% and reduced the cleaning efficiency to 96.63%. These results indicate that the air separation performance first improves and then declines with increasing inlet air velocity, demonstrating that the inlet air velocity must be appropriately selected rather than excessively high or low. The numerical simulation results are summarized in Table 4, and the variation trends of cleaning efficiency, impurity rate, and loss rate are plotted in Fig. 12.

Table 4

Inlet air velocity (m/s)	Impurity rate (%)	Loss rate (%)
15	11.65	2.46
16	6.75	0.55
17	1.59	0.26
18	1.82	1.55

Numerical simulation results under different inlet air velocities

In summary, variations in inlet air velocity do not significantly alter the overall flow field structure inside the air separation chamber, but they have a substantial influence on the particle separation performance. Considering the impurity rate, loss rate, and cleaning efficiency across the four inlet air velocity conditions, it can be concluded that, at an airflow inclination angle of 21° and a feeding rate of 2000 particles/s, inlet air velocities in the range of 16–18 m/s provide satisfactory cleaning performance. Among them, an inlet air velocity of 17 m/s yields the optimal separation effect under the current parameter conditions.

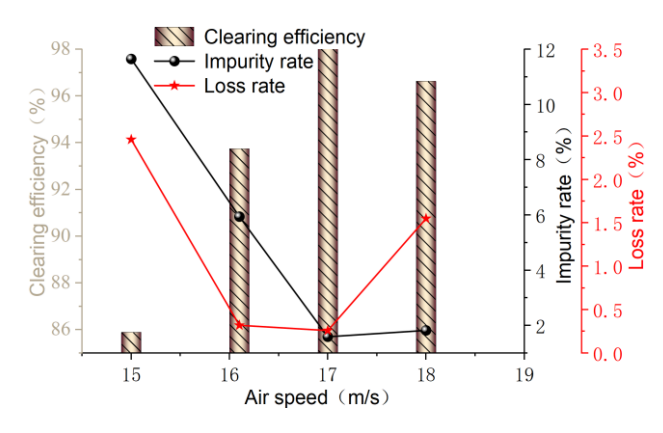


Fig. 12 - Variation of impurity rate, loss rate, and cleaning efficiency under different inlet air velocities

Influence of air inlet width on soybean air winnowing performance

As shown in Fig. 13, particle motion snapshots were obtained at an airflow inclination angle of 21° and inlet air velocities corresponding to air inlet widths of 160 mm, 190 mm, 220 mm, and 250 mm. As the inlet width increases, the airflow volume entering the chamber increases accordingly, causing the particle movement position to shift forward, which can be observed from the changing collision positions between the plump large soybeans and the baffle. When the inlet width is 160 mm, the particle travel distance is too short, resulting in some material failing to reach its designated outlet. In contrast, when the inlet width is 250 mm, the particle travel distance becomes excessive, causing plump large soybeans to mix with underdeveloped small soybeans at the wrong outlet. Therefore, to ensure accurate particle classification, the inlet width must be appropriately selected, rather than too small or too large.

Fig. 14 shows the particle force distribution and airflow velocity contours at an airflow inclination angle of 21°, a feeding rate of 2000 particles/s, and air inlet widths of 160 mm, 190 mm, 220 mm, and 250 mm. As shown in the figure, the maximum airflow velocity near the inlet corner first increases and then decreases as the inlet width increases. Although the overall airflow pattern in the air separation chamber remains generally unchanged, the region in which particles experience dominant aerodynamic force gradually shifts forward with increasing inlet width. This shift is the primary reason why the particle travel distance increases as the inlet width becomes larger.

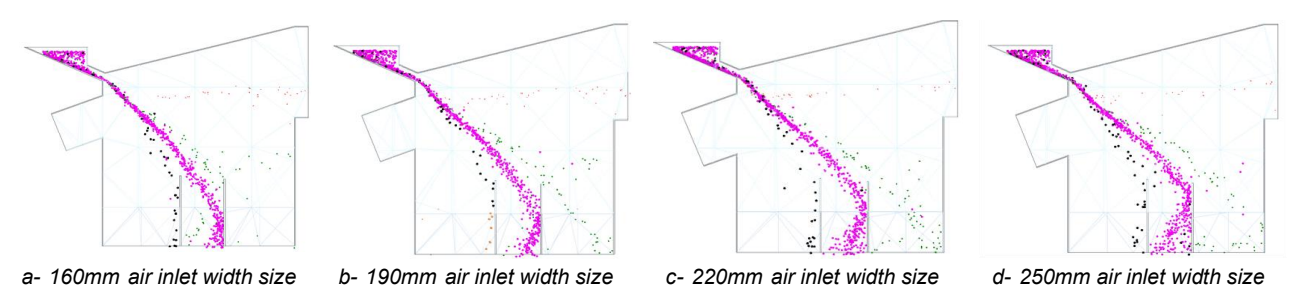


Fig. 13 - Particle motion snapshots under different air inlet widths

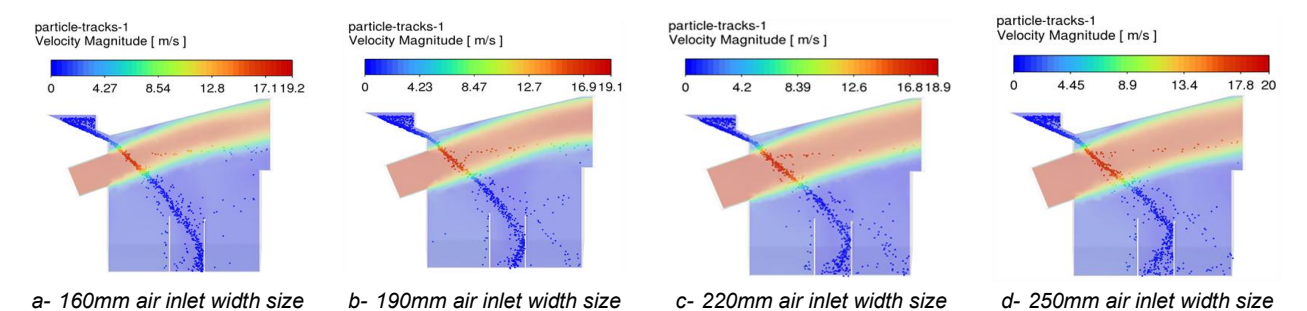


Fig. 14 - Particle force distribution and airflow velocity contours under different air inlet widths

As shown in Table 5, increasing the air inlet width results in a continuous decrease in impurity rate, while the loss rate decreases initially and then increases. This observation is consistent with the previous analysis of particle trajectories and particle force distribution within the airflow field. As the inlet width increases, the airflow volume entering the separation chamber increases, leading to greater particle flight height and forward movement. This enables particles to fall more accurately into their designated outlets, thereby reducing the impurity rate. However, when the inlet airflow becomes excessive, plump large soybeans continue to be carried forward beyond their intended separation region, causing the loss rate to rise again. Therefore, an appropriate air inlet width must be selected to maintain both low impurity rate and low loss rate, ensuring optimal cleaning efficiency. To clearly illustrate these trends, the variation curves of cleaning efficiency, impurity rate, and loss rate are plotted in Fig. 15.

In summary, increasing the air inlet width expands the airflow region inside the air separation chamber, although the overall flow pattern remains essentially unchanged. However, the air inlet width has a significant influence on particle separation performance. Considering the impurity rate, loss rate, and cleaning efficiency across the four inlet width conditions, it can be concluded that, at an airflow inclination angle of 21° and a feeding rate of 2000 particles/s, air inlet widths in the range of 190–250 mm yield satisfactory cleaning performance. Among these, an inlet width of 220 mm provides the best separation effect under the current operating conditions.

Table 5
Numerical simulation results under different air inlet widths

Air inlet width mm)	Impurity rate (%)	Loss rate (%)
160	9.94	0.51
190	3.18	0.35
220	1.59	0.26
250	1.46	0.70

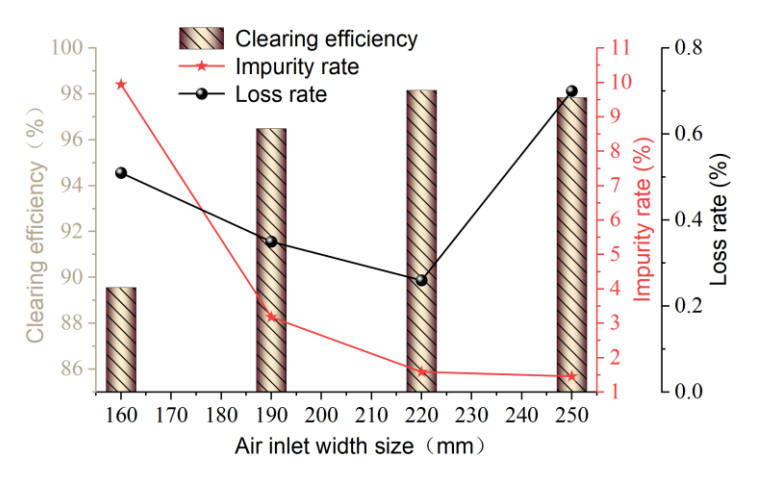


Fig. 15 - Variation of impurity rate, loss rate, and cleaning efficiency under different air inlet widths

Combining the above simulation results, the optimal air separation performance is achieved when the inlet air velocity is 17 m/s, the airflow inclination angle is 21°, and the air inlet width is 220 mm, under the control variable method. Under these conditions, the impurity rate is 1.59%, the loss rate is 0.26%, and the cleaning efficiency reaches 98.15%.

CONCLUSIONS

- (1) Based on a comparative analysis of horizontal and inclined airflow separation methods, and considering the physical characteristics and separation requirements of the soybean mixture, the inclined airflow separation method was selected. Accordingly, a tilted air-winnowing chamber model was established to evaluate separation performance.
- (2) The SN52 soybean mixture was classified into four particle categories, and a simulation particle model was constructed using measured physical parameters. Contact parameters, including restitution coefficients and static and rolling friction coefficients for particle-particle and particle-acrylic interactions, were determined through experiments and previous research, providing the necessary data foundation for the CFD-DEM coupled simulation.
- (3) Using the CFD–DEM coupling approach and a single-factor control method, the effects of airflow inclination angle, inlet air velocity, and air inlet width on soybean separation performance were analyzed. The optimal separation performance was achieved at an air velocity of 17 m/s, inclination angle of 21°, and air inlet width of 220 mm, resulting in an impurity rate of 1.59%, loss rate of 0.26%, and cleaning efficiency of 98.15%.

REFERENCES

- [1] Chen Wudong, Zhao Yan, Wen Haijiang, Ying W. (2019). Research on soybean roasting storage and selection processing technology (大豆烘储及精选加工工艺研究) [J]. *Modern Agriculture*, 2019(08): 71-72. https://doi.org/10.3969/j.issn.1001-0254.2019.08.039
- [2] Chen Guangwei, Li Fuxing, Qu FaYi, Zhang C.J. (2024). Parameter calibration and experiment of discrete element simulation of spherical-like soybean based on DEM [J]. *INMATEH-Agricultural Engineering*, 74(3):303-315. https://doi.org/10.35633/inmateh-74-26
- [3] Du Xiaoqiang, Xiao Menghua, Hu Xiaoqin, Chen Jianneng, Zhao Yun. (2014). Numerical simulation and experiment of gas-solid two-phase flow in cross-flow grain cleaning device (贯流式谷物清选装置气固两相流数值模拟与试验) [J]. *Transactions of the Chinese Society of Agricultural Engineering*, 30(3): 35-42. https://doi.org/10.3969/j.issn.1002-6819.2014.03.004
- [4] Hu Zhizheng, Zeng Haifeng, Ge Yun, Wang Wendong, Wang Jiangkun. (2021). Simulation and Experiment of Gas-Solid Flow in a Safflower Sorting Device Based on the CFD-DEM Coupling Method[J]. Processes, 9 (7): 1239-1239. https://doi.org/10.3390/pr9071239
- [5] Krzysiak Z., Samociuk W., Zarajczyk J., Kaliniewicz Z., Pieniak D., Bogucki M. (2020). Analysis of the Sieve Unit Inclination Angle in the Cleaning Process of Oat Grain in a Rotary Cleaning Device. *Processes*, 8(3):346. https://doi.org/10.3390/pr8030346
- [6] Moses J A, Jayas D S, Alagusundaram K. (2014). Simulation and validation of airflow pressure patterns for horizontal airflow through bulk canola [J]. *Journal of Agricultural Engineering*, 51(04): 2385-2391. https://doi.org/10.52151/jae2014514.1561
- [7] Nahal A.M., Arabhosseini A., Kianmehr M.H. (2013). Separation of shelled walnut particles using pneumatic method [J]. *International Journal of Agricultural and Biological Engineering*, 6(3):88-93. https://doi.org/10.3965/j.ijabe.20130603.0011
- [8] Toomer, O.T., Oviedo, E.O., Ali, M., Patino, D., Joseph, M., Frinsko, M., Vu, T., Maharjan, P., Fallen, B., Mian, R. (2023). Current Agronomic Practices, Harvest & Post-Harvest Processing of Soybeans (Glycine max)—A Review. *Agronomy*, 13(2): 427. https://doi.org/10.3390/agronomy13020427
- [9] Tsuji Y, Kawaguchi T, Tanaka T. (1993). Discrete particle simulation of two-dimensional fluidized bed [J]. *Powder technology*, 77(1): 79-87. https://doi.org/10.1016/0032-5910(93)85010-7
- [10] Thiet Xuan Nguyen, Lu Minh Le, Thong Chung Nguyen, Nguyen Thi Hanh Nguyen, Tien Thinh Le, Binh Thai Pham, Vuong Minh Le, Hai Bang Ly. (2020). Characterization of soybeans and calibration of their DEM input parameters[J]. *Particulate Science and Technology*, 39 (5): 1-19. https://doi.org/10.1080/02726351.2020.1775739
- [11] Xie Guangfan. (2022). Application of blast air separator in municipal waste classification (鼓风式风选机在 城市垃圾分类中的应用) [J]. *Mechanical & Electrical Engineering Technology*, 51(03): 264-266. https://doi.org/10.3969/j.issn.1009-9492.2022.03.058
- [12] Zhao Feng, Yuan Ruibo, Li Xi. (2021). Numerical simulation of tobacco leaf fluid motion trajectory based on Fluent simulation (基于 Fluent 仿真的烟叶流体运动轨迹数值模拟) [J]. *Agricultural Equipment & Vehicle Engineering*, 59(09): 59-63+68. https://doi.org/10.3969/j.issn.1673-3142.2021.09.013

- [13] Zhao Lei, Ma Xuedong, Guo Bingjiang, Yu Haichuan. (2020). Simulation study of grain cleaning based on DEM-CFD coupling (基于 DEM-CFD 耦合的谷物清选模拟研究) [J]. *Journal of Shandong Agricultural University (Natural Science Edition*), 51(04):738-743. https://doi.org/10.3969/j.issn.1000-2324.2020.04.033
- [14] Zhang Dejun, Zhang Xiaoming, Wu Di, Lin Shuyun, Zhang Taihua. (2023). Simulation study of pepper cleaning based on DEM-CFD coupling (基于 DEM-CFD 耦合的辣椒清选仿真研究) [J]. *Journal of Agricultural Science and Technology*, 25(07): 87-96. https://doi.org/10.13304/j.nykjdb.2022.0008
- [15] Zhu Huajiang, Zhang Sihao, Wang Wenjun, Lv Hongqian, Chen Yulong, Zhou Long, Li Mingwei, Zhao Jinhui. (2024). Design and Testing of Soybean Double-Row Seed-Metering Device with Double-Beveled Seed Guide Groove [J]. *Agriculture*, 14 (9): 1595-1595. https://doi.org/10.3390/agriculture14091595